Particulate emissions from laser ignited and spark ignited hydrogen fueled engines

Article *in* International Journal of Hydrogen Energy · June 2017

DOI: 10.1016/j.ijhydene.2017.04.031

INTERNATIONAL JOURNAL OF HYDROGEN ENERGY 42 (2017) 15956–15965

Available online at www.sciencedirect.com

ScienceDirect

journal homepage: www.elsevier.com/locate/he

Particulate emissions from laser ignited and spark ignited hydrogen fueled engines

*Akhilendra Pratap Singh, Anuj Pal, Neeraj Kumar Gupta, Avinash Kumar Agarwal**

Engine Research Laboratory, Department of Mechanical Engineering, Indian Institute of Technology Kanpur, Kanpur, 208016, India

A R T I C L E I N F O

Article history:
Received 13 September 2016
Received in revised form
31 March 2017
Accepted 5 April 2017
Available online 2 June 2017

Keywords:
Laser ignition
Spark ignition
Particulate number-size distribution
Nucleation and accumulation mode particles
Particulate mass-size distribution

A B S T R A C T

Exponentially increasing energy demand and stricter emission legislations have motivated researchers to explore alternative fuels and advanced engine technologies, which are more efficient and environment friendly. In last two decades, hydrogen has emerged as promising alternative fuel for internal combustion (IC) engines and vehicles. For gaseous fuels, laser ignition (LI) has emerged as a novel ignition technique due to its superior characteristics, leading to improved combustion, engine performance and emission characteristics. Numerous advantages of LI system such as flexibility of plasma location, lower NO_x emissions and capability of igniting ultra-lean fuel–air mixture makes LI system superior compared to conventional spark ignition (SI) system. This study experimentally compares particulate emissions from hydrogen fueled engine ignited by LI and SI systems. Experiments were performed in a constant speed engine prototype, which was suitably modified to operate on gaseous fuels using both LI as well as SI systems. Particulate were characterized using engine exhaust particle sizer (EEPS) spectrometer. Results showed that LI engine resulted in relatively higher particulate number concentration as well as particulate mass compared to SI engine. In both ignition systems, particulate emissions increased with increasing engine load however rate of increase was relatively higher in LI system. Relatively larger count mean diameter (CMD) of particulate emitted from SI engine compared to LI engine was another important observation. This showed emission of relatively smaller particles in larger numbers from LI engine, compared to baseline SI engine.

Introduction

Conventional diesel engines are used in various light and heavy-duty applications due to higher power output, higher brake thermal efficiency (BTE) and greater robustness compared to their gasoline counterparts. However, emission of different toxic gaseous species and carbonaceous particulate matter (PM) limit their applications. To control harmful emissions and to comply with prevailing emission regulations, automotive industry is exploring the possibility of deploying advanced combustion techniques such as homogeneous charge compression ignition (HCCI) [1], premixed charge compression ignition (PCCI) [2] etc., in addition to using after-treatment devices such as diesel oxidation catalysts

* Corresponding author.
E-mail address: akag@iitk.ac.in (A.K. Agarwal).

http://dx.doi.org/10.1016/j.ijhydene.2017.04.031

(DOC) [3], diesel particulate filter (DPF) [4] etc. and deploying alternative fuels such as biofuels [5–9], gaseous alternate fuels [10–13] etc. in IC engines. These steps reduce engine out emissions significantly however increased complexity and cost of vehicles remain the major issues of these techniques. On the other side, rapid depletion of non-renewable petroleum reserves is alarming and automotive industry needs to explore alternative energy resources for sustaining the burgeoning transport sector. To resolve this, researchers are focusing on using alternative fuels in transport sector such as biodiesel [5–8], straight vegetable oils (SVOs) [9], primary alcohols [8], compressed natural gas (CNG) [10], hydrogen [11], hydrogen-CNG (HCNG) mixtures [12], liquefied petroleum gas (LPG) [13], etc. Amongst these alternative fuels, most fuels have a common concern of particulate emissions, which have harmful effects on the human health [14,15].

Particulate formation in the engine combustion chamber can be reduced by homogeneous fuel–air mixing [16]. Therefore researchers performed experiments using gaseous fuels, which resulted in homogeneous fuel–air mixture due to their higher diffusivity [10–13]. They reported that use of gaseous fuels results in lower particulate mass emission however particulate number concentration still cannot be neglected. They suggested that presence of carbon atoms in the fuels is the main reason for particulate formation. Therefore zero/low carbon fuels such as hydrogen, dimethyl ether (DME) and CNG are very attractive and have also been explored [17]. Amongst these test fuels, hydrogen has been found to be most suitable fuel for IC engines due to its superior properties and ultra-low emission potential. Hydrogen is an odorless, non-toxic and renewable alternative fuel, which can be produced through electrolysis of water, gasification of coal, biomass and steam reformation of natural gas [18]. Hydrogen combustion produces only water vapors as combustion product therefore it can be a potentially a promising sustainable alternative fuel candidate for next generation engines. Several researchers experimentally verified improved combustion, engine performance and emission characteristics of hydrogen. Gatts et al. [19] reported that addition of hydrogen along with conventional fuels led to improved performance and ultra-low emissions at high loads. Singh et al. [20] carried out engine experiment using mineral diesel, gasoline, CNG, HCNG and hydrogen and reported that hydrogen fueled engine emitted the lowest particulate numbers as well as particulate mass amongst all test fuels. However, significant number of particulate emitted by gaseous fuels is another concern because relatively smaller size particles emitted by gaseous fuels increase the associated health risk. To investigate the source of particulate from zero-carbon fuels, Singh et al. [20] carried out a comprehensive study and suggested that all particulate were not formed due to combustion of fuel alone. Significant amount of particulate were formed due to incomplete combustion of lubricating oil as well. Organ-metallic additives in the lubricating oil undergo evaporation during combustion and they condense during cooling of exhaust gas, resulting in formation of various organic and inorganic compounds getting adsorbed on particulate surfaces [21]. During post-combustion reactions, these compounds act as soot precursors and promote particulate formation. Khalek et al. [21] reported that engines with lower particulate emissions favored by re-nucleation of lubrication oil additives in the exhaust, lead to higher particulate emissions. Significant contribution to the particulate emission from lubricating oil pyrolysis was also reported by Zielinska et al. [22]. They reported that the polycyclic aromatic hydrocarbons (PAHs) emissions from gasoline engines showed greater similarity with the composition of PAHs present in the lubricating oil rather than gasoline. Influence of particle size on human health has also increased scientific curiosity in other measures of particulate emissions such as their size, number and surface area. Relatively smaller particles (D_p < 50 nm) have more severe impact on human health compared to relatively larger particles (D_p > 100 nm). Smaller particles have higher probability to be inhaled and deposited in the human respiratory tract and alveolar region by diffusion [23]. Toxicological studies have shown that fine particles (D_p < 2.5 μm) have higher toxicity per unit mass of particulate, compared to coarse particles (D_p < 10 μm) [23].

Apart from particulate emissions, Pal et al. [24], Dharamshi et al. [25], and Das [26] reported that pre-ignition and backfire of hydrogen engine leads to excessive noise at higher engine loads. These issues could be resolved by using an electrode-less ignition system for igniting the hydrogen–air mixtures in the engine combustion chamber. Previous studies showed that the slight variation in fuel properties, method of ignition and engine operating conditions significantly affect particulate characteristics [20]. Therefore it becomes necessary to investigate particulate emission characteristics of laser ignited (LI) engines. LI system is a novel concept used for ignition of fuel–air mixture inside the combustion chamber. LI is an electrode-less ignition system, which inhibits probability of auto-ignition and backfire in hydrogen fueled engine. In LI, a pulsating laser beam is converged at the focal point using a converging lens. This focused laser beam with high energy density at the focal point of the converging lens creates plasma. Plasma is formed only when the energy density at the focal point breaches the threshold value. Other than controlling backfire and auto-ignition, LI has emerged as a superior ignition technique capable of delivering superior engine performance and emissions. In previous studies, advantages of LI system such as lower NO_x emissions, higher power output and ignition capability of ultra-lean fuel–air mixture have been reported [24–28]. However particulate emission characteristics of hydrogen fueled LI engines have not been investigated thoroughly. Therefore this study aims to explore differences in particulate characteristics of a hydrogen fueled engine ignited with LI system and a conventional spark plug. The experiments were performed in a constant speed engine prototype at five different engine loads (5, 10, 15, 20 and 25 Nm) using hydrogen as test fuel. All other parameters such as spark timing and engine compression ratio were kept constant for both ignition systems.

Experimental setup

In this study, experiments were performed on a constant speed diesel engine (Kirloskar; DM10) prototype suitably modified to operate in SI and LI modes. For all experiments, compression ratio was kept constant at 11.0. Ignition timing was maintained fixed at 23° bTDC for both ignition systems. Table 1 shows the important specifications of the original and modified test engine.

For hydrogen utilisation, the original diesel engine was modified and a prototype engine was developed to operate in SI mode, as shown in Fig. 1.

Engine modifications included several hardware modifications along with integrating electronic circuits, which control ignition timing and port fuel injector. Due to safety issues related to hydrogen, development of suitable fuel injection system was the most critical task. Hydrogen has very fast flame speed, therefore it has a tendency of backfiring in the intake manifold. The intensity of hot spots in the combustion chamber could be minimized by suitably developing an appropriate fuel injection strategy. A Coriolis force based mass flow meter (Emerson, CMF010M) measured the mass flow rate of hydrogen being inducted into engine manifold. Hydrogen requires very low ignition energy for initiating combustion therefore engine backfire can occur, primarily due to hot spots present in the engine combustion chamber. In the event of backfire, flames can propagate rapidly from the inlet manifold towards the gas cylinders, and can possibly cause a catastrophic explosion. In order to avoid such unwanted accident, several safety measures were adapted in this experimental setup. Two safety devices were designed and fabricated, namely a flame arrestor and a flame trap. Flame arrester was used for quenching the flames propagating backwards by arresting them in the device. Flame trap used water trap for quenching the flames traveling backwards. The fuel line was connected to a high volume flow rate solenoid injector (Alternative Fuel Systems, Gs-60-05-5 H), downstream of these safety devices. This solenoid injector was specifically designed for injection of gaseous fuels into the intake manifold of the engine. To control the fuel injection parameters, a dedicated electronic circuit was designed. This circuit controls all fuel injection parameters such as timing of start of injection, injection duration (thus fuel injection quantity) and injection lag. Fuel injection duration was devised in a way to inject entire fuel quantity when the intake valve remained open i.e. during the intake stroke. This was done in order to ensure that fuel residuals were not left in the intake manifold for the next cycle, which might possibly trigger a backfire, when the intake valve opens in the next engine cycle. During the experiment, the engine loads were varied by altering the fuel injection duration (i.e. by altering the amount of fuel injected by the injector).

Experiments were repeated again using LI system under identical operating conditions, in order to compare the characteristics of particulate generated by SI and LI systems. For installing the LI system, the existing SI system was suitably modified and a Q-switched Nd: YAG laser (Litron, Nano L-200-30) of 1064 nm wavelength was installed in the experimental setup (Fig. 2).

In this setup, electrical spark plug system was replaced with a laser spark plug system [24,26,28]. LI system consists of a collimating unit (a combination of diverging and collimating lenses) and a beam reflector. The collimating unit was used mainly for increasing the laser beam diameter and the beam reflector was mainly used to direct the laser beam in to the laser spark plug, which was installed in the engine cylinder head. The angle of laser beam reflector could be adjusted such that the laser beam is aligned parallel to the axis of laser spark plug. Laser spark plug houses a lens holder, which contains a converging lens for generating laser plasma at its focal point, which is located inside the combustion chamber of the engine. To seal the combustion chamber, a sapphire window was housed in the end of the laser spark plug. This window allows only the laser beam from the laser spark plug to pass to the combustion chamber. A dedicated customized laser triggering circuit was designed, which triggers the laser at 23° bTDC in the compression stroke, similar to a conventional SI system.

For measurement of particulate number-size distribution, an engine exhaust particle sizer (EEPS) spectrometer (TSI Inc.; EEPS-3090) was used. This equipment provides both high temporal resolution and a reasonable size resolution by employing multiple detectors, which work in parallel. EEPS was capable of measuring particle sizes ranging from 5.6 nm to 560 nm, having a maximum concentration up to 10^8 particles/cm^3 in the engine exhaust. To avoid error of over

Table 1 – Specifications of test engine.

Specifications	Original diesel engine	Hydrogen spark ignition (modified)	Hydrogen laser ignition (modified)
Make/Model	Kirloskar/DM-10	Kirloskar/DM-10 (modified)	Kirloskar/DM-10 (modified)
Injection type	Direct injection	Port fuel injection	Port fuel injection
Number of cylinders		One	
Ignition type	Compression ignition	Spark ignition	Laser ignition
Spark timing (°bTDC)		NA	
Bore (mm)/stroke (mm)		102/116	
Displaced volume (cc)		948	
Compression ratio	17.5	11	11
Connecting rod length (mm)		232	
Intake air		Naturally Aspirated	
Inlet valve opening		4.5° bTDC	
Inlet valve closing		35.5° aBDC	
Exhaust valve opening		35.5° bBDC	
Exhaust valve closing		4.5° aTDC	
Cooling system		Water cooled	

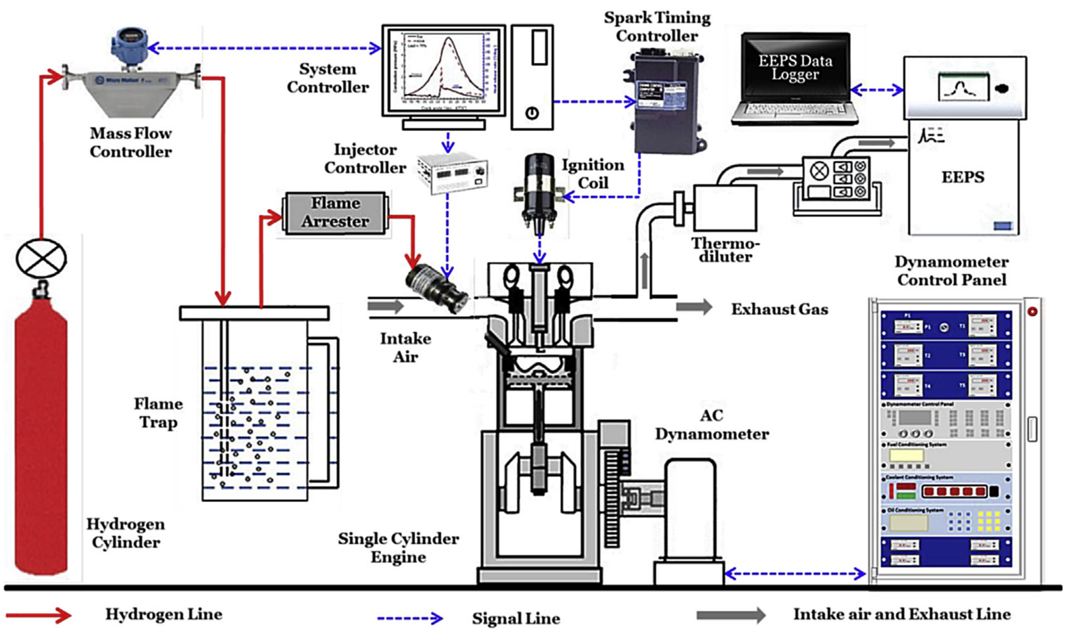

Fig. 1 – Experimental setup of hydrogen fueled SI engine.

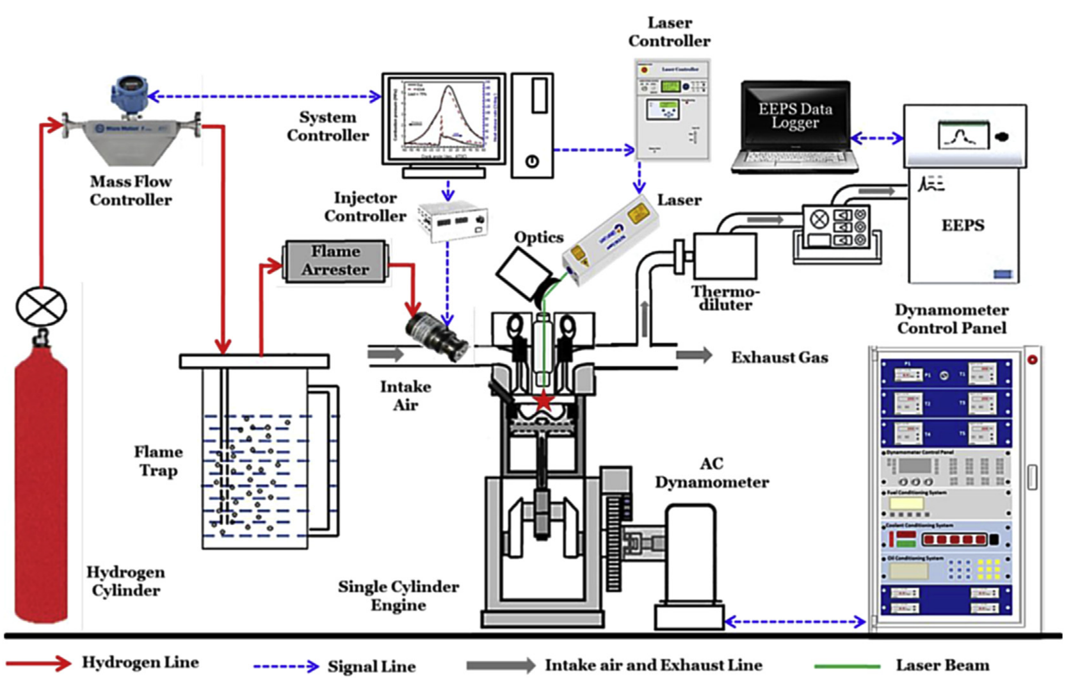

Fig. 2 – Experimental setup of hydrogen fueled LI engine.

concentration of particulate, a rotating disk thermo-diluter (Matter Engineering; MD19-2E) was used, which diluted the exhaust gas 115 times before it entered the EEPS for particulate number-size distribution measurement. To remove particles larger than $D_p > 1\ \mu m$, exhaust gas was passed through a cyclone with cut-off diameter of 1 μm, just upstream of EEPS. Working principle and details of EEPS are detailed in the instrument manual [29].

Results and discussion

Present experimental study shows comparative particulate characteristics of hydrogen fueled engine ignited with LI system as well as conventional SI system. For comparing particulate emissions, all experiments were performed at 1500 rpm under identical experimental conditions at five different engine loads/torques (5, 10, 15, 20, and 25 Nm). Exhaust sampling was done after thermal stabilization of the engine in each test condition. At each operating condition, particulate samples were measured for 1 min at a sampling frequency of 1 Hz i.e. each data set was recorded 60 times. Average of these 60 data sets at one experimental condition was further analyzed and the results were presented with standard deviation as the error bar.

Particulate number-size distribution

Fig. 3 shows the number-size distribution of particulate emitted by hydrogen fueled engine at different engine loads. Results showed that hydrogen fueled engine also emitted significant number of particulate in the exhaust, which cannot be neglected.

In hydrogen fueled engine, particulate formation primarily takes place due to incomplete combustion of lubricating oil present on the combustion chamber walls. Heavier molecules of lubricating oil with long carbon-chain length don't burn completely and convert into unburned hydrocarbons (HCs) and PAHs. During post-combustion reactions, these compounds generate soot precursors, leading to particulate formation. From Fig. 3, it can be noted that for both LI and SI systems, nucleation mode particle (NMP) (i.e. particle diameter D_p < 50 nm) concentration was relatively higher compared to the accumulation mode particle (AMP) (i.e. particle diameter 50 nm < D_p < 1000 nm) concentration.

Particulate emission trends for both LI and SI are similar at all loads. At 25 Nm, NMP concentration was significantly higher compared to other loads. This was mainly due to presence of relatively larger hydrogen quantity in the engine cylinder, which resulted in higher heat release rate (HRR). This increased the lubricating oil pyrolysis and resulted in higher NMP concentration. At higher engine loads, combustion duration also shortened due to relatively faster fuel–air combustion kinetics, which prevented coagulation of particulate, resulting in higher NMP concentration. Significantly higher particulate emissions from LI system compared to SI system was an important finding of this study.

In LI system, laser beam has significantly higher optical frequency compared to plasma frequency therefore laser beam can propagate into the interiors of the plasma kernel. However SI system operates at a significantly lower frequency compared to plasma frequency, therefore the electrical energy cannot propagate deeper inside the plasma and the plasma is sustained by absorption within a thin layer near the plasma surface in this case [24,30]. For this reason, the pressure and temperature generated by LI plasma are significantly higher (~10^3 bar and 10^6 K respectively) [24,30–32] by an order of magnitude compared to SI plasma (~10^2 bar and 10^4 K respectively) [33,34]. This was primarily due to these intense conditions, LI resulted in relatively earlier SoC of the hydrogen–air mixture in the combustion chamber, leading to relatively higher in-cylinder temperatures compared to SI system. Higher in-cylinder temperature increased the pyrolysis of larger lubricating oil quantity, leading to higher particulate emissions. Higher ignition energy in LI engine encouraged volumetric combustion, which resulted in higher particulate

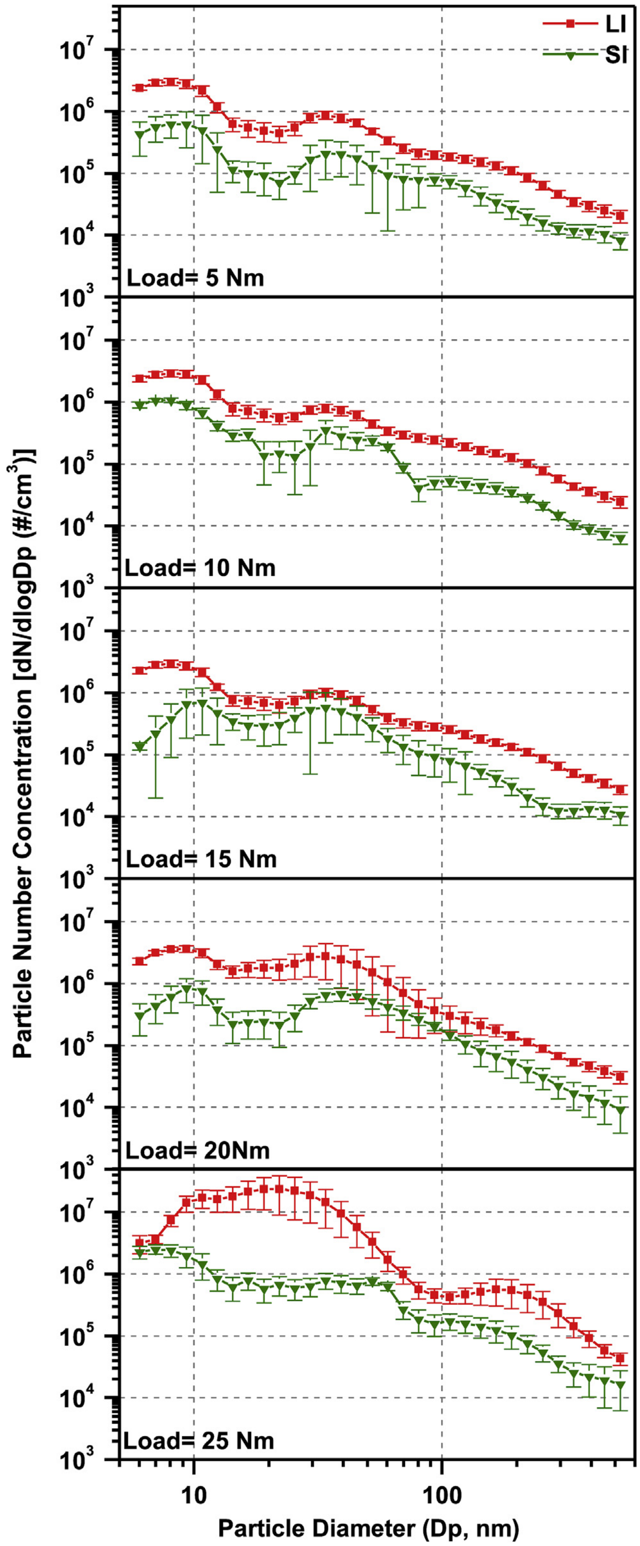

Fig. 3 – Number-size distribution of particulate emitted by hydrogen fueled SI and LI engine at different engine loads.

nuclei generation during combustion. This led to higher NMP concentration from LI engine compared to SI engine. Incomplete combustion of lubricating oil also led to formation of different types of organic and inorganic compounds, which condensed on to the particulate nuclei during the expansion stroke. These condensates were also adsorbed onto the surface of primary particulate and resulted in formation of higher number of AMP. The number concentration of AMP also increased due to in-cylinder pyrolysis of lubricating oil, which encouraged formation of larger particles. Lower numbers of AMP in SI engine suggested relatively less dominant particulate formation and condensation of organic species onto them.

Presence of two peaks in number-size distribution of particulate emitted by LI and SI engines was another important observation. These peaks correspond to NMP and AMP. In case of LI engine, peak corresponding to AMP reduced with increasing engine load (up to 15 Nm) however in case of SI engine, peak corresponding to AMP increased slightly (up to 20 Nm) with increasing engine load. This showed that increasing fuel quantity was more effective in particulate formation in SI engine compared to LI engine. In LI engine, particulate emission was predominantly affected by ignition mechanism however in case of SI engine, overall combustion affected the particulate emissions predominantly.

Nucleation and accumulation mode particle concentrations

Fig. 4 shows the comparison of NMP and AMP number concentrations emitted by LI and SI engines. For both engines, NMP number concentration slightly increased with increasing engine load. Higher in-cylinder temperatures due to combustion of relatively larger fuel quantity was the main reason for this trend in both cases. Results showed that LI engine resulted in significantly higher NMP number concentration compared to SI engine. This was mainly due to significantly higher energy density of LI plasma compared to SI plasma. This led to superior combustion at higher in-cylinder temperature inside the combustion chamber, resulting in higher combustion efficiency, which led to pyrolysis of greater lubricating oil quantity in case of LI system compared to SI system.

Fig. 4 also shows that NMP number concentration was significantly higher compared to AMP concentration. This was

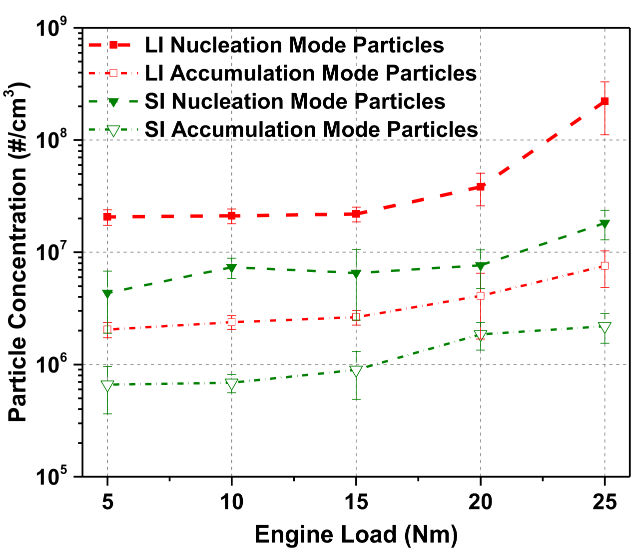

Fig. 4 – Number concentrations of nucleation and accumulation mode particulate emitted from hydrogen fueled SI and LI engines at varying engine loads.

caused by two factors. First was the higher nucleation tendency due to incomplete combustion of lubricating oil and the second one was relatively shorter combustion duration (faster flame speed) of hydrogen–air mixtures. This prevented coagulation of smaller particulate and led to relatively lesser AMP concentration. Similar to NMP, AMP number concentration also increased with increasing engine load. This trend was however common for both ignition systems. In LI engine, AMP number concentration was relatively higher compared to SI engine. Higher NMP number concentration and formation of more volatile organic species were the two factors responsible for this trend.

Total particle number concentration and count mean diameter

Fig. 5(a) shows the total particle number (TPN) concentration from hydrogen fueled LI and SI engines. Both engines showed that TPN concentration slightly increased with increasing engine load. Rate of increase in TPN concentration also increased at higher engine load. Higher TPN concentration at higher engine load was mainly due to higher amount of hydrogen inducted into the combustion chamber, which resulted in higher HRR and higher in-cylinder temperature that encouraged pyrolysis of lubricating oil. At 25 Nm, TPN concentration increased significantly vis-à-vis lower loads. This observation was in agreement with particulate number-size distribution. Results showed that TPN concentration was significantly higher in LI engine (2×10^7–2×10^8 particles/cm^3 of exhaust gas) compared to SI engine (5×10^6–2×10^7 particles/cm^3 of exhaust gas). At 25 Nm load, LI engine showed significantly higher increase in TPN compared to SI engine. This was mainly due to combined increase in NMP and AMP concentrations (Fig. 4).

Fig. 5(b) shows the count mean diameter (CMD) of particulate at varying engine loads for both LI and SI engines. CMD was calculated from the particulate number-size distribution using the following equation.

$$CMD = \frac{n_1 d_1 + n_2 d_2 + n_3 d_3 + \ldots\ldots + n_n d_n}{n_1 + n_2 + n_3 + \ldots\ldots n_n}$$

Here n_i is the particulate number concentration corresponding to diameter D_i. CMD represents the weighted arithmetic average of the particulate. Lower CMD shows dominance of smaller particulates, which leads to relatively higher risk to human health.

For both engines, CMD of particulate increased with increasing engine load however rate of increase of CMD was relatively higher in case of SI engine. At 25 Nm, both engines showed a substantial reduction in CMD. This was mainly attributed to significantly higher NMP number concentration. At very high engine load, relatively faster fuel–air combustion kinetics reduced total combustion duration. This inhibited coagulation of newly formed particulate and resulted in significantly lower CMD of particulate. Fig. 5(b) showed that CMD of particulate emitted by SI engine (~26–40 nm) was relatively higher compared to LI engine (~25–30 nm). This was attributed to relatively lower HRR in SI engine, and provided more time for particulate coagulation, leading to higher CMD of particulate.

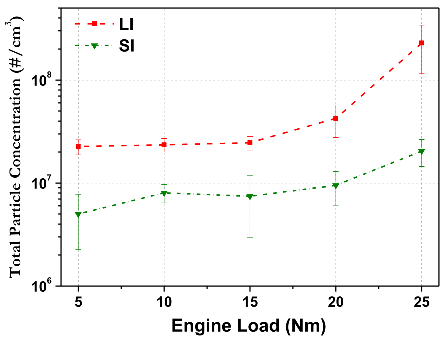

(a) Total Particulate Concentration

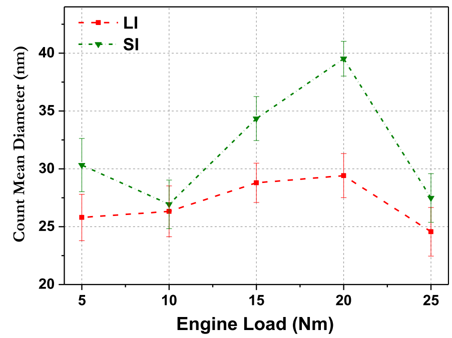

(b) Count Mean Diameter

Fig. 5 – TPN concentration and CMD of particulate emitted by hydrogen fueled SI and LI engines at varying engine loads.

Particulate surface area-size distribution

Particulate surface area is an important parameter to characterize engine particulate. Particulate surface area represents the surface area available for adsorption of PAHs and volatile hydrocarbon species on to the particulate. Higher surface area poses greater risk due to higher surface adsorption of toxic species, which when inhaled into the human body through the respiratory system, may lead to life threatening diseases and health conditions. Particulate surface area can be calculated from the particulate number-size distribution, by assuming particulate to be spherical [35].

$$dS = dN \cdot (D_p)^2$$

In this equation, dS is the area concentration of particles with size range having mean diameter D_p; and dN is the number concentration of particulate with mean diameter D_p.

Fig. 6 shows the comparative surface area-size distribution of particulate emitted by LI and SI engines.

In both engines, particulate surface area increased with increasing particulate size. This showed that contribution of bigger particles was higher in total particulate surface area. Higher surface area of bigger particles showed relatively lower risk to human health because bigger particles tend to get trapped in upper tracts of the respiratory system. For both engines, particulate surface area increased with increasing engine load. Surface area of particulate emitted by LI engine was relatively higher compared to that of SI engine. Surface area-size distribution also showed higher particulate surface area in nucleation mode size range. This led to synergistic combination of two harmful effects of higher surface area available for adsorption of toxic hydrocarbons, and lower particulate size distribution, which tends to penetrate deeper into the human respiratory system, thereby causing greater harm to human health.

Particulate mass-size distribution

Particulate mass-size distribution is another important parameter to understand effect of particulate on human health and environment. In terms of environmental hazards, heavier particles are relatively less harmful compared to lighter particles due to their shorter retention time in the atmosphere. Heavier particles tend to settle rather quickly compared to lighter particles, which tend to float around in the atmosphere for a longer time. Hence heavier particles have lower probability to be inhaled into the human respiratory system. Fig. 7 shows mass-size distribution of particulate emitted by hydrogen fueled LI and SI engines. Particulate mass was calculated from the particulate number-size distribution, assuming them to be spherical particles with constant density (1 g/cm^3) [29,35]. The particles emitted in the engine exhaust have varied shapes and sizes but they are considered spherical because these particles were primarily formed of agglomerates.

Similar to surface area-size distribution, mass-size distribution of particulate also increased with increasing particle size. Results showed that particulate mass increased with increasing engine load. At higher engine loads, greater fuel quantity was inducted, which promoted pyrolysis of lubricating oil due to higher in-cylinder temperature (higher HRR).

Particulate mass was also relatively higher for LI engine compared to SI engine. This showed that in LI system, larger lubricating oil quantity was pyrolyzed, which resulted in higher particulate mass emission. Particulate mass-size distribution also showed that LI engine emitted higher number of particulate in AMP size range. Therefore even though NMPs contain 60–70% of total particulate number emissions, it doesn't contribute significantly to particulate mass. AMPs were generated mainly due to condensation of heavier organic species on the primary particles.

Nucleation and accumulation mode particulate mass

Fig. 8 shows the particulate mass corresponding to NMP and AMP. It was calculated from the particulate mass-size distribution. Results showed that particulate mass corresponding to both NMP and AMP increased with increasing engine load. Rate of increase in particulate mass was higher for NMP compared to AMP. Contrary to NMP and AMP concentration, mass distribution showed slightly different trend. Results showed that particulate mass corresponding to AMP was significantly higher compared to NMP. This was mainly due to higher contribution of larger particles in particulate mass. Higher mass of particulate emitted from LI engine was another important observation. This was due to higher particle emissions from LI engine in both nucleation mode and accumulation mode, which resulted in higher particulate mass.

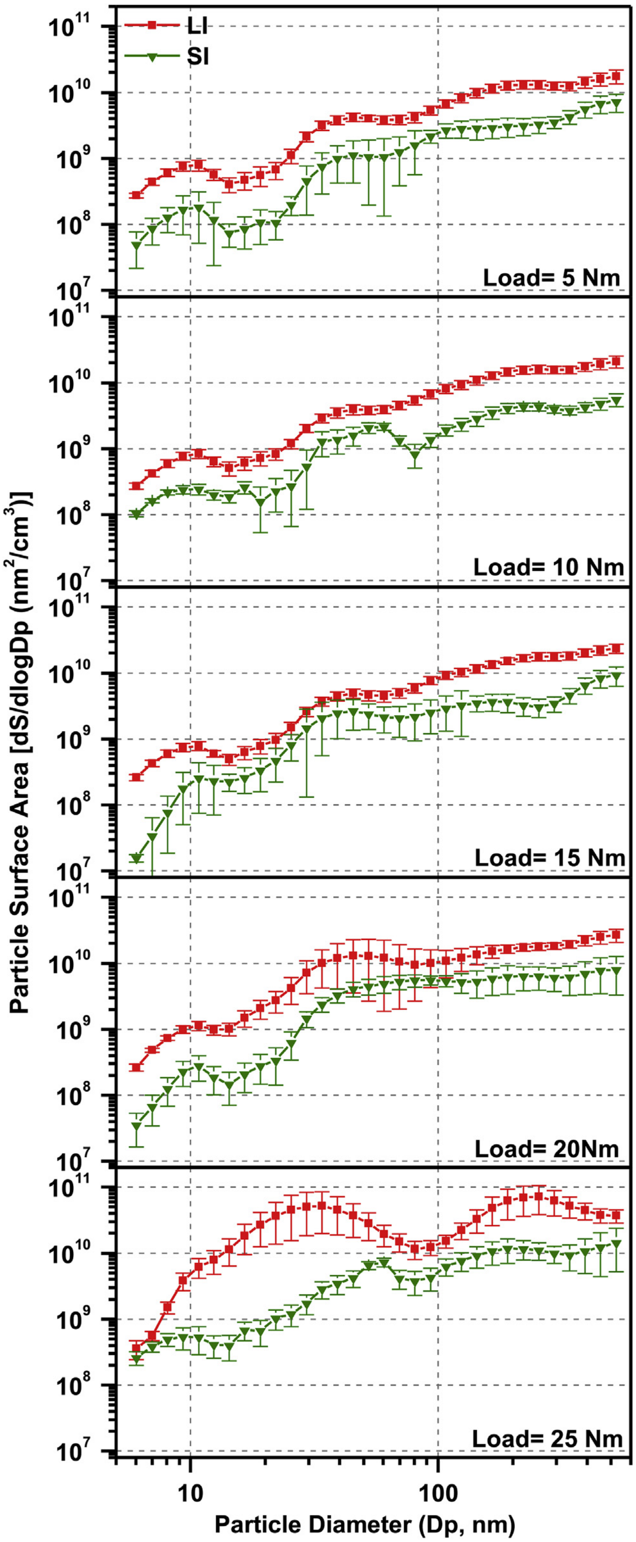

Fig. 6 – Surface area-size distributions of particulate emitted by hydrogen fueled SI and LI engines at varying engine loads.

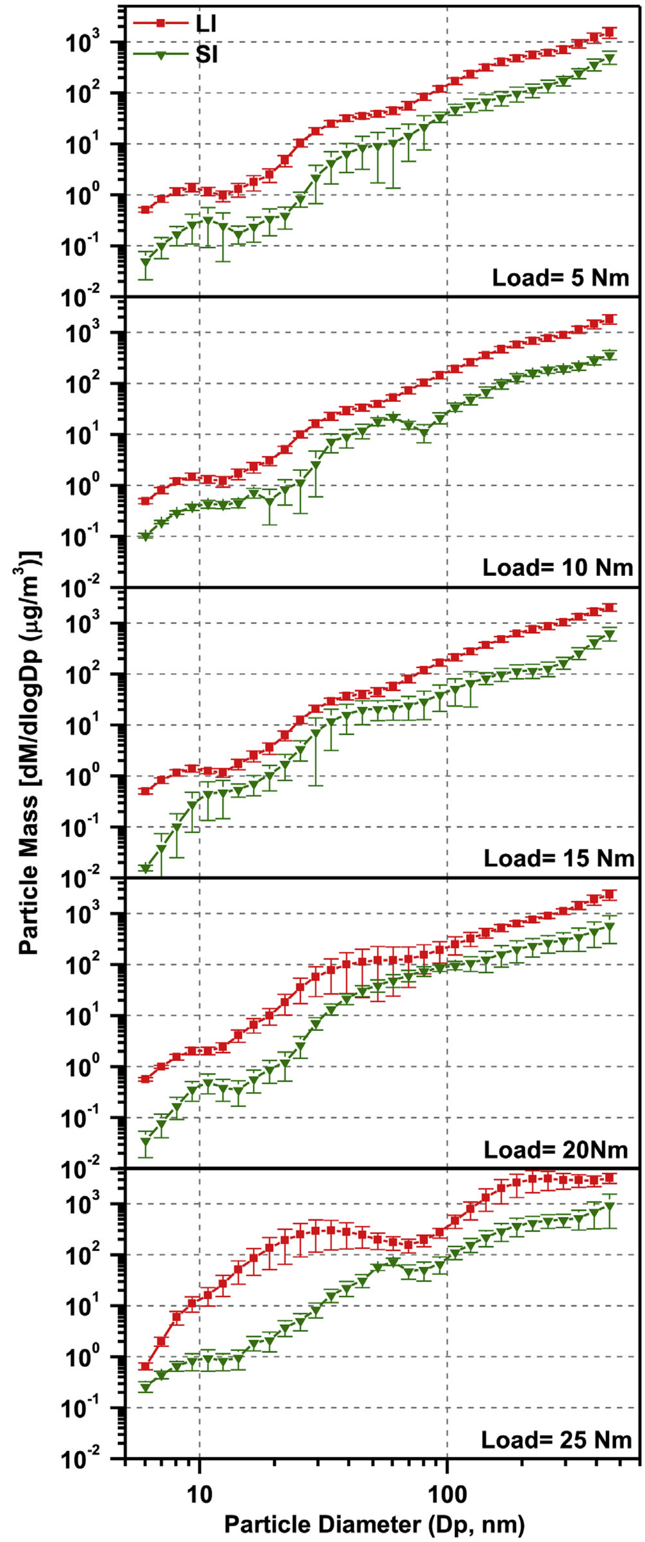

Fig. 7 – Mass-size distribution of particulate emitted by hydrogen fueled SI and LI engines at varying engine loads.

Total particulate mass

Fig. 9 shows total particle mass (TPM) emitted from LI and SI engines.

Results showed that TPM increased slightly with increasing engine load. At 25 Nm, TPM increased drastically due to presence of higher fuel quantity in the combustion chamber, which increased the HRR. Comparison of TPM

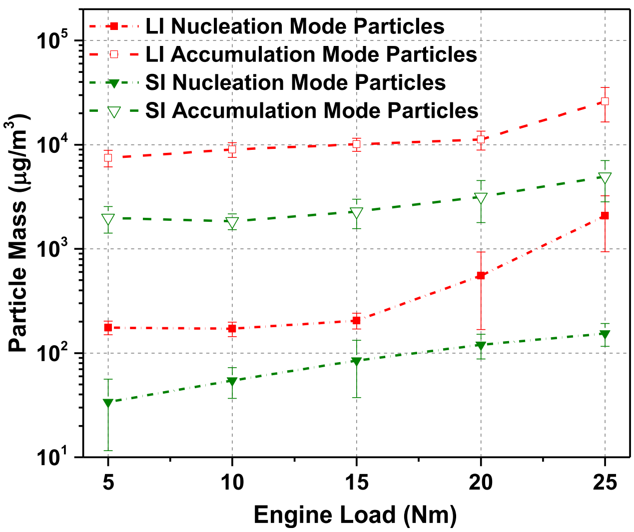

Fig. 8 – Nucleation and accumulation mode particulate mass emitted by hydrogen fueled SI and LI engines at varying engine loads.

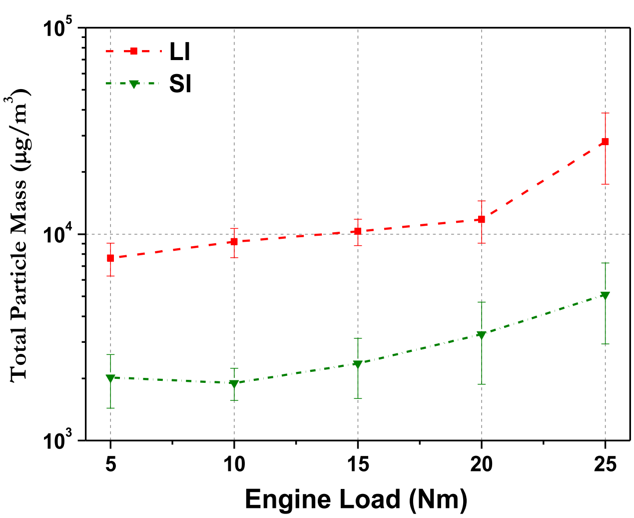

Fig. 9 – Total particulate mass emitted by hydrogen fueled SI and LI engines at varying engine loads.

trends of LI and SI engines showed that TPM of LI engine (~8 × 10^3 to 3 × 10^4 μg/m^3 of exhaust gas) was significantly higher compared to SI engine (~2 to 4 × 10^3 μg/m^3 of exhaust gas). This was mainly due to relatively higher in-cylinder temperature and pressure, which led to pyrolysis of lubricating oil present inside the combustion chamber. Higher TPM was another important observation. It validated the previous results as well and showed that the tendency of incomplete combustion was higher in LI engine compared to SI engine.

Conclusions

This experimental study showed the comparison of particulate characteristics emitted by a hydrogen fueled engine, which was ignited by conventional spark ignition system and a newly developed laser ignition system. Experiments were performed in a constant speed engine prototype at varying engine loads. To compare the particulate characteristics, experiments were performed at identical engine operating conditions. Results showed that the particulate number concentration in case of LI engine was significantly higher compared to SI engine. Higher HRR in LI engine was the main reason for this trend, which increased the tendency of incomplete combustion/pyrolysis of lubricating oil. Particulate size classification showed that both NMP and AMP concentrations were higher in LI engine compared to SI engine. However in both cases, NMP concentration was significantly higher compared to AMP. Particulate surface area-size distribution was also higher in LI engine. This indicates greater adsorption of toxic organic species onto the particulate surface, thus posing greater risk for human health. For both engines, particulate mass increased with increasing engine load however LI engine emitted relatively higher particulate mass compared to SI engine. CMD of particulate emitted by the LI engine was smaller compared to SI engine, which indicated relatively deeper lung penetration potential of these particulate.

Overall, it can be concluded that although LI system is beneficial in terms of engine performance, however its particulate toxicity is possibly higher compared to SI engine. For improving the particulate characteristics emanating from LI engine, thermal stability of lubricating oil should be improved, so that incomplete combustion/pyrolysis of lubricating oil can be reduced.

Acknowledgements

Financial support from Council for Scientific and Industrial Research (CSIR), Government of India's SRA scheme to Dr. Akhilendra Pratap Singh is acknowledged, which supported his stay at ERL, IIT Kanpur for conducting these experiments.

REFERENCES

[1] Singh AP, Agarwal AK. Fuel vaporizer: a potential solution for HCCI combustion of low volatile fuels. Energy Fuels 2017;31(3):3164–81.
[2] Jain A, Singh AP, Agarwal AK. Effect of split fuel injection and EGR on NOx and PM emission reduction in a low temperature combustion (LTC) mode diesel engine. Energy 2017;122:249–64.
[3] Shukla PC, Gupta T, Labhsetwar NK, Agarwal AK. Development of low cost mixed metal oxide based diesel oxidation catalysts and their comparative performance evaluation. RSC Adv 2016;6(61):55884–93.
[4] Fernández JR, Lapuerta M, Valdepeñas JS. Regeneration of diesel particulate filters: effect of renewable fuels. Renew Energy 2017;104:30–9.
[5] Shukla PC, Gupta T, Agarwal AK. A comparative morphological study of primary and aged particles emitted from a biodiesel (B20) vis-à-vis diesel fueled CRDI engine. Aerosol Air Qual Res 2014;14(3):934–42.
[6] Singh G, Singh AP, Agarwal AK. Experimental investigation of combustion, performance and emission characterization

of biodiesel fueled HCCI engine using external mixture formation technique. Sustain Energy Technol Assess 2014;6:116–28.
[7] Dhar A, Agarwal AK. Effect of Karanja biodiesel blends on engine wear in a transportation engine. Fuel 2014;134:81–9.
[8] Agarwal AK. Bio-fuels (alcohols and biodiesel) applications as fuels for internal combustion engines. Prog Energy Combust Sci 2007;33(3):233–71.
[9] Agarwal AK, Dhar A. Wear, durability and lubricating oil performance of a straight vegetable oil (Karanja) blend fueled DICI engine. J Renew Sustain Energy 2012;4:1–13.
[10] Hora TS, Agarwal AK. Effect of varying compression ratio on combustion, performance, and emissions of a hydrogen enriched compressed natural gas fueled engine. J Nat Gas Sci Eng 2016;31:819–28.
[11] Dharamshi K, Agarwal AK. Parametric study of a laser ignited hydrogen–air mixture in a constant volume combustion chamber. Int J Hydrogen Energy 2014;39(35):20207–15.
[12] Hora TS, Agarwal AK. Experimental study of the composition of hydrogen enriched compressed natural gas on engine performance, combustion and emission characteristics. Fuel 2015;160:470–8.
[13] Aravind B, Kishore VR, Mohammad A. Combustion characteristics of the effect of hydrogen addition on LPG–air mixtures. Int J Hydrogen Energy 2015;40(46):16605–17.
[14] Samet JM, Dominici F, Curriero FC, Coursac I, Zeger SL. Fine particulate air pollution and mortality in 20 U.S. cities, 1987–1994. N Engl J Med 2000;343:1742–9.
[15] Dockery DW, Pope CA, Xu X. An association between air pollution and mortality in six US cities. N. Engl J Med 1993;329:1753–9.
[16] Agarwal AK, Dhar A, Srivastava DK, Maurya RK, Singh AP. Effect of fuel injection pressure on diesel particulate size and number distribution in a CRDI single cylinder research engine. Fuel 2014;107:84–9.
[17] Muradov NZ, Veziroğlu TN. "Green" path from fossil-based to hydrogen economy: an overview of carbon-neutral technologies. Int J Hydrogen Energy 2008;33(23):6804–39.
[18] Hydrogen Production. U.S. Department of Energy [cited on 25.06.14].
[19] Gatts T, Li H, Liew C, Liu S, Spencer T, Wayne S, et al. An experimental investigation of H_2 emissions of a 2004 heavy-duty diesel engine supplemented with H_2. Int J Hydrogen Energy 2010;35(20):11349–56.
[20] Singh AP, Pal A, Agarwal AK. Comparative particulate characteristics of hydrogen, CNG, HCNG, gasoline and diesel fueled engines. Fuel 2016;185:491–9.
[21] Khalek AI, Kittelson DB, Graskow BR, Wei Q, Brear F. Diesel exhaust particle size: measurement issues and trends. 1998. SAE paper 980525.
[22] Zielinska B, Sagebiel J, Mcdonald DJ, Whitney K, Lawson DR. Emission rates and comparative chemical composition from selected in-use diesel and gasoline-fueled vehicles. J Air Waste Manage Assoc 2004;54:1138–50.
[23] Pope III CA, Thun MJ, Namboodiri MM, Dockery DW, Evans JS, Speizer FE, et al. Particulate air pollution as a predictor of mortality in a prospective study of U.S. adults. Am J Respir Crit Care Med 1995;151:669–74.
[24] Pal A, Agarwal AK. Comparative study of laser ignition and conventional electrical spark ignition systems in a hydrogen fuelled engine. Int J Hydrogen Energy 2015;40(5):2386–95.
[25] Dharamshi K, Pal A, Agarwal AK. Comparative investigations of flame kernel development in a laser ignited hydrogen–air mixture and methane–air mixture. Int J Hydrogen Energy 2013;38(25):10648–53.
[26] Das LM, Dutta V. Hydrogen energy activities in India. Int J Hydrogen Energy 2015;40(11):4280–3.
[27] O'Brianta SA, Gupta SB, Vasu SS. Review: laser ignition for aerospace propulsion. Propuls Power Res 2016;5(1):1–21.
[28] Pal A, Agarwal AK. Effect of compression ratio on combustion, performance and emissions of a laser ignited single cylinder hydrogen engine. Int J Hydrogen Energy 2015;40(36):12531–40.
[29] Engine exhaust particle sizer™ spectrometer model 3090. TSI, USA: Operation and Service Manual; March 2009.
[30] Radziemski LJ, Cremers D. Laser-induced plasmas and applications. New York: Marcel Dekker Inc; 1989.
[31] Phouc TX, White FP. Laser-induced spark ignition of CH_4/Air mixtures. Combust Flame 1999;119(3):203–16.
[32] Phuoc TX. Laser spark ignition: experimental determination of laser-induced breakdown thresholds of combustion gases. Opt Commun 2000;175(4–6):419–23.
[33] Heywood JB. Internal combustion engine fundamentals. Nueva York: McGraw Hill; 1989.
[34] Maly R, Vogel M. Initiation and propagation of flame fronts in lean CH4 e air mixtures by the three modes of the ignition spark. In: Proceedings of seventeenth international symposium on combustion; 1976. p. 821–31.
[35] Gupta T, Kothari A, Srivastava DK, Agarwal AK. Measurement of number and size distribution of particles emitted from a mid-sized transportation multipoint port fuel injection gasoline engine. Fuel 2010;89(9):2230–3.